Robust Cooperative Control of Networked Train Platoons: A Negative-Imaginary Systems' Perspective

Chunyu Li, Jianan Wang, *Senior Member, IEEE*, Jiayuan Shan, Alexander Lanzon, *Senior Member, IEEE*, and Ian R. Petersen, *Fellow, IEEE*

***Abstract*—By virtue of the wide implementation of communication-based train control (CBTC) systems and moving-block signaling systems, cooperative control for trains shows great potential in improving line utilization, passenger comfort, and operation flexibility. However, the operation of train platoons faces great challenges induced by model uncertainties, unpredictable resistances, and time-varying disturbances. To address these problems, consensus-based robust cooperative control schemes are presented in this article for both homogeneous and heterogeneous train platoons. Taking the physical connection between carriages into consideration, each train in the platoon is modeled as a negative-imaginary (NI) system, and the NI property is rigorously proved in this article. In the foundation of cooperative control theories of NI systems, robust strictly NI controllers considering the network topology are utilized to track a predefined motion reference. The proposed controllers are robust to both mass uncertainties and external disturbances. Moreover, the line utilization for the railway system and the ride comfort for the passengers are improved using the proposed control schemes. Numerical simulations are given to showcase the effectiveness and robustness of the proposed controllers.**

***Index Terms*—Communication-based train control (CBTC) systems, moving-block signaling (MBS) systems, multiple train coordination, negative imaginary (NI) systems, robust cooperative control.**

Manuscript received December 8, 2020; revised March 7, 2021; accepted April 13, 2021. Date of publication May 26, 2021; date of current version December 3, 2021. This work was supported by the National Natural Science Foundation of China under Grant 61873031. Recommended by Associate Editor S. L. Smith. *(Corresponding author: Jianan Wang.)*

Chunyu Li, Jianan Wang, and Jiayuan Shan are with the School of Aerospace Engineering, Beijing Institute of Technology, Beijing 100081, China (e-mail: 3120195051@bit.edu.cn; wangjianan@ieee.org; sjy1919@bit.edu.cn).

Alexander Lanzon is with the Control Systems Centre, Department of Electrical and Electronic Engineering, School of Engineering, University of Manchester, Manchester M13 9PL, U.K. (e-mail: Alexander.Lanzon@manchester.ac.uk).

Ian R. Petersen is with the Research School of Engineering, Australian National University, Canberra, ACT 2601, Australia (e-mail: i.r.petersen@gmail.com).

Digital Object Identifier 10.1109/TCNS.2021.3084064

I. Introduction

COMMUNICATION-BASED train control (CBTC) systems have been widely implemented in modern railway systems around the world. Based on CBTC, the position, velocity, and acceleration information of trains can be accurately detected and transmitted to onboard and ground control systems with very low latency, and the permitted speed is, then, calculated and transmitted back to the trains enabling safe, comfortable, and efficient operation of the railway system. This dynamic way of determining the moving authority of trains shows huge potential in improving running density on the railway. The coordination between trains becomes significant in these circumstances and has attracted extensive interest from the research community to develop robust and effective controllers [1]–[4].

In this article, by virtue of graph theory and negative-imaginary (NI) theory, the robust formation control problem for train platoons is addressed. Roughly speaking, NI systems with transfer function $G(s)$ are systems with an NI frequency response, which denotes $j[G(j\omega) - G(j\omega)^*] \geq 0$. Since it was initially proposed in [5], it has been widely implemented in a variety of fields including large space structures, flexible robotic arms, and nanopositioning systems [6], [7]. In [8], NI theory is applied to address the string stability of a vehicle platoon. However, the results are limited to single-input single-output systems for their continued fractions property. For the multiple-input multiple-output (MIMO) case, cooperative control schemes for networked heterogeneous and homogeneous NI systems have been studied in [9] and [10], respectively. In this article, by modeling the trains in a platoon as multiple NI systems, the output feedback consensus is implemented to train coordination, and the robustness is also inherited from stability theories of NI systems.

Due to the complicated operation environment of trains, i.e., unpredictable resistances, various weathers, track gradients, and line curves, the robustness of cooperative train controllers is still a challenging problem. The uncertain characteristics of trains are studied in [11], where an adaptive cooperative control method with only one parameter requiring online tuning is proposed. To further eliminate the dependence on resistance coefficients, a control scheme using prescribed performance function is introduced in [12] for cooperative train control. The control approaches for virtual coupling of railway trains are studied

in [13]. In the literature mentioned before, each train is modeled as a point-mass system, ignoring the structure of a train in reality. In contrast with them, our method is particularly suitable for the trains in an electric multiple unit (EMU) configuration, which has been widely used in suburban and high-speed trains around the world, including the China Railway High-speed, Shinkansen in Japan and ICE 3 in Germany. An EMU train consists of multiple self-propelled units, and each unit is composed of a carriage with a traction motor and one or more carriages without power. Since the driving power source of EMU is distributed compared with the traditional locomotive-hauled trains, EMU trains are treated as MIMO systems with NI property in this article, allowing the implementation of relative NI theories.

To address the position and velocity tracking problem of EMU trains, a data-driven control algorithm is investigated, which avoids the precise modeling of the train dynamics and complicated system identification [14]. Considering the physically connected subsystems, a distributed and fault-tolerant control method is proposed in [15]. The difficulty of modeling train dynamics motivates the application of machine learning on a heavy haul train with a distributed power configuration in [16]. Nevertheless, the train with multiple carriages in [14]–[16] is still treated as one single controlled object, which does not consider the cooperative control for multiple trains in a platoon under the moving-block signaling (MBS) system. Although cooperative control of multiple EMU trains is studied in [17], the heterogeneous situation is not considered, which is included in our work.

In summary, the main contributions of this article are listed from two perspectives, which are as follows.

1) New model: A more precise train dynamic model is utilized for describing trains compared to the point-mass model. Using this model, the controllers are capable of driving each unit separately, which shows better practicality for EMU trains. The consensus achieved between units can improve the ride comfort of passengers. The mass variation of each train is also considered simulating the passengers' variation in reality.
2) New control: The proposed homogeneous and heterogeneous controllers can realize robust formation tracking for train platoons under external disturbances and mass uncertainties, guaranteed by the related stability theories of NI and strictly NI (SNI) interconnection systems. The line efficiency can also be improved via maintaining the formation of the train platoon in a minimum safety interval.

The remaining of this article is organized as follows. Preliminaries on graph theory and NI theory are provided in Section II. In Section III, dynamic models and NI properties of train platoons systems are presented, and the control objectives are also described. Section IV presents control methods for the homogeneous case with corresponding experimental results. In Section V, the cooperative control problem for the heterogeneous case is addressed along with experimental validation. A conclusion is drawn in Section VI.

The notation in this article is standard. $\mathbb{R}$ denotes the set of real numbers, whereas $\mathbb{C}$ denotes the set of complex numbers. $[P, Q]$ denotes the positive feedback interconnection between systems P and Q. $A \otimes B$ denotes the Kronecker product of the two matrices A and B. $\mathcal{L}_N \in \mathbb{R}_{N\times N}$ denotes the Laplacian matrix of a graph with N nodes. G^* denotes complex conjugate transpose of matrix G. $\mathrm{Ker}(\mathcal{L}_N)$ denotes kernel of the Laplacian matrix. I_n denotes the identity matrix with dimension of $n \times n$, whereas $\mathbf{1}_n$ denotes the vector of all ones with dimension of $n \times 1$. In addition, $\mathrm{diag}_{i=1}^{n}\{A_i\}$ is a diagonal matrix with $A_i, i \in \{1, \ldots, n\}$ on the diagonal.

II. Preliminaries on Graph Theory and NI Systems Theory

A. Graph Theory

Graph theory can be utilized to describe the interactive relationships among a group of agents. A graph $\mathcal{G} = (\mathcal{V}, \varepsilon)$ consists of a set of vertices $\mathcal{V} = \{v_1, v_2, \ldots, v_n\}$ with n nodes, and a set of edges $\varepsilon = \{(v_i, v_j) \in \mathcal{V} \times \mathcal{V}\}$ with l edges. $\mathcal{A} = \{a_{ij}\} \in \mathbb{R}^{N\times N}$ is the adjacency matrix where the adjacency a_{ij} from j to i equals 0 if $j = i$. Also, $a_{ij} = 1$ if $(v_i, v_j) \in \varepsilon$ and 0 otherwise. For an undirected graph, $a_{ij} = a_{ji}$. Define the in-degree matrix $\Delta = \mathrm{diag}_{i=1}^{N}\{\Delta_i\}$ where $\Delta_i = \sum_{j=1}^{N} a_{ij}$ is the in-degree of node i. The Laplacian matrix of the graph is, then, defined as $\mathcal{L}_n = \Delta - \mathcal{A}$. Define the $n \times l$ incidence matrix $\mathcal{Q}$ of $\mathcal{G}$ with elements q_{ij} as follows:

$$\begin{cases} q_{ij} = 1, & \text{if } i \text{ is the initial vertex of edge } j \\ q_{ij} = -1, & \text{if } i \text{ is the end vertex of edge } j \\ q_{ij} = 0, & \text{otherwise.} \end{cases}$$

It is well known that the relationship between the incidence matrix and the Laplacian matrix of an undirected and connected graph $\mathcal{G}$ is $\mathcal{L}_n = \mathcal{Q}\mathcal{Q}^T$, and

$$\mathcal{L}_n \geq 0, \mathrm{Ker}(\mathcal{L}_n) = \mathrm{Ker}(\mathcal{Q}^T) = \mathrm{span}\{\mathbf{1}_n\}. \tag{1}$$

B. NI Systems Theory

Since the control systems designed for train platoons in this article are based on NI theories, the following introduces the NI and SNI definitions and the corresponding stability theory.

Definition 2.1 (see [6]): A square, real, rational, and proper transfer function $G(s)$ is NI if the following conditions are satisfied:

1) $G(s)$ has no pole in $\mathrm{Re}[s] > 0$;
2) for all $\omega > 0$ such that $j\omega$ is not a pole of $G(s)$, $j(G(j\omega) - G(j\omega)^*) \geq 0$;
3) if $s = j\omega_0$ where $\omega_0 > 0$ is a pole of $G(s)$, then it is a simple pole and the residue matrix $K = \lim_{s\to j\omega_0}(s - j\omega_0)jG(s)$ is Hermitian and positive semidefinite;
4) if $s = 0$ is a pole of $G(s)$, then $\lim_{s\to 0} s^k G(s) = 0$ for all $k \geq 3$ and $G_2 = \lim_{s\to 0} s^2 G(s)$ is Hermitian and positive semidefinite.

Definition 2.2 (see [5]): A square, real, rational, and proper transfer function $G_s(s)$ is SNI, if the following conditions are satisfied:

1) $G_s(s)$ has no pole in $\mathrm{Re}[s] > 0$;
2) for all $\omega > 0, j(G_s(j\omega) - G_s(j\omega)^*) > 0$.

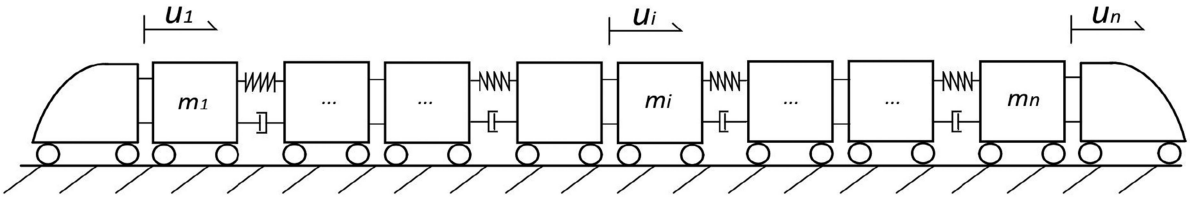

Fig. 1. Train composed of n physically connected units with spring–damper couplers.

Lemma 2.1 (see [18]): Given a transfer function $S_1 = \begin{bmatrix} 0 & I_n \\ I_n & P \end{bmatrix} \in \mathbb{C}_{a\times a}$ and a transfer function $S_2 = Q \in \mathbb{C}_{n\times n}$ where $a = 2n$. If both S_1 and S_2 are NI, and the Redheffer Star product $S_1 \star S_2 = Q(I_n - PQ)^{-1}$ is internally stable, $S_1 \star S_2$ is also NI.

The results in [6] extend the definition of NI systems to include free-body dynamics and also provide necessary and sufficient conditions for stability of corresponding feedback systems. The following constant matrices are defined to derive stability conditions:

$$\begin{aligned} G_2 &= \lim_{s\to 0} s^2 G(s) \\ G_1 &= \lim_{s\to 0} s(G(s) - G_2/s^2) \\ G_0 &= \lim_{s\to 0} (G(s) - G_2/s^2 - G_1/s). \end{aligned} \tag{2}$$

These matrices are the first three coefficients in the Laurent series expansion of the system transfer function [6]. The properties of the free-body dynamics are included in these matrices defined before, which are utilized to describe stability conditions for the positive feedback interconnection of NI and SNI systems. For $G_2 \neq 0$, define a decomposed full-column rank matrix satisfying $G_2 = JJ^T$. Suppose $G_1 = 0$ and $J^T G_s(0) J$ is non-singular, then define the matrix N_2 as

$$N_2 = G_s(0) - G_s(0)J(J^T G_s(0) J)^{-1} J^T G_s(0). \tag{3}$$

Lemma 2.2 (see [6]): Given a strictly proper NI plant $G(s)$ with $G_2 \neq 0$ and a connected SNI controller $G_s(s)$ with $J^T G_s(0) J$ being nonsingular. Suppose $G_1 = 0$, then the positive feedback interconnection system $[G(s), G_s(s)]$ is internally stable if and only if

$$J^T G_s(0) J < 0 \tag{4}$$

and either

$$I - N_2^{\frac{1}{2}} G_0 N_2^{\frac{1}{2}} > 0 \tag{5}$$

when $N_2 \geq 0$ or

$$det(I + \widetilde{N}_2 G_0 \widetilde{N}_2) \neq 0 \tag{6}$$

when $N_2 \leq 0$. Here, $\widetilde{N}_2 = (-N_2)^{\frac{1}{2}}$.

III. Problem Formulation

A. Dynamics for EMU Trains

The dynamics model for EMU trains is explained in this section. Considering the carriages within a unit are usually permanently coupled together, the connections between them are assumed to be solid in our model. By applying Newton's second law, the dynamics of a train with n units, as shown in Fig. 1, can be described using the following equations:

$$\begin{cases} m_1 \ddot{p}_1 = -k(p_1 - p_2) - c(\dot{p}_1 - \dot{p}_2) + u_1 \\ \qquad\qquad \vdots \\ m_i \ddot{p}_i = k(p_{i-1} - p_i) - k(p_i - p_{i+1}) \\ \qquad +c(\dot{p}_{i-1} - \dot{p}_i) - c(\dot{p}_i - \dot{p}_{i+1}) + u_i \\ \qquad\qquad \vdots \\ m_n \ddot{p}_n = k(p_{n-1} - p_n) + c(\dot{p}_{n-1} - \dot{p}_n) + u_n \end{cases} \tag{7}$$

where $i \in \{2, 3, \ldots, n-1\}$ and m_i, k, and c denote the mass of each unit, stiffness coefficient, and damping coefficient of the connecting couplers, respectively. $p_i, i \in \{1, 2, \ldots, n\}$ is the position of each unit. To verify the NI property of the train system, the transfer function is derived

$$\begin{cases} p_1(s) = \dfrac{1}{m_1 s^2}[u_1(s) - (k + cs)(p_1 - p_2)] \\ \qquad\qquad \vdots \\ p_i(s) = \dfrac{1}{m_i s^2}[u_i(s) - (k + cs)(p_i - p_{i-1}) \\ \qquad\qquad - (k + cs)(p_i - p_{i+1})] \\ \qquad\qquad \vdots \\ p_n(s) = \dfrac{1}{m_n s^2}[u_n(s) - (k + cs)(p_n - p_{n-1})]. \end{cases} \tag{8}$$

Inductively, we find that the transfer function of a train with an arbitrary number $n \geq 2$ of coupled units can be expressed in the following way:

$$\boldsymbol{y(s)} = [M(s) - T(s)\mathcal{L}_{t_n}]^{-1} \boldsymbol{u}(s) \tag{9}$$

where $M(s) = \text{diag}_{i=1}^{n}\{m_i s^2\}$ and $T(s) = -(k + cs)$ represent the mass matrix and couplers, respectively, and $\boldsymbol{y(s)} = [p_1(s), p_2(s), \ldots, p_n(s)]^T$ and $\boldsymbol{u(s)} = [u_1(s), u_2(s), \ldots, u_n(s)]^T$ are the output and input vectors, respectively. For an EMU train, since each unit is connected only to the neighboring ones, their relationship can be described via an undirected and connected graph, from which the Laplacian matrix $\mathcal{L}_{t_n}$ can be derived.

We define the matrix $M_x(s) = \text{diag}_{i=1}^{n}\{\tilde{m}_i s^2\}$ where $\tilde{m}_i$ is the possibly maximum mass of each unit, thus the transfer

function in such a scenario is

$$G_x(s) = [M_x(s) - T(s)\mathcal{L}_{t_n}]^{-1}. \tag{10}$$

To represent the changing mass caused by passengers getting on and off the train, a changing ratio d $(0 < d < 1)$ is introduced. Suppose that the mass of each unit changes proportionally, the mass matrix becomes $M(s) = dM_x(s)$, and the general transfer function described by $M_x(s)$ is

$$\begin{aligned} G(s) &= [M(s) - T(s)\mathcal{L}_{t_n}]^{-1} \\ &= [dM_x(s) - T(s)\mathcal{L}_{t_n}]^{-1}. \end{aligned} \tag{11}$$

Although $G(s)$ is not linear with $G_x(s)$, it is found that their coefficients constant matrices defined in (2) are linear. Suppose that the constant matrices G_2, G_1, and G_0 correspond to $G(s)$, and G_{2_x}, G_{1_x}, and G_{0_x} correspond to $G_x(s)$. Then, their relationships are derived as follows:

$$\begin{aligned} G_2 &= \left(\frac{1}{\sum_{i=1}^{n} m_i}\right)_{n\times n} = \left(\frac{1}{d\sum_{i=1}^{n} \tilde{m}_i}\right)_{n\times n} = \frac{1}{d}G_{2_x} \\ G_1 &= G_{1_x} = \mathbf{0}, \qquad G_0 = G_{0_x}. \end{aligned} \tag{12}$$

These properties will be utilized to analyze the effect of mass uncertainties on the stability in the following controller design section.

B. NI Property of Train Systems

The proof of the NI nature of a single train with n units is provided in this section. It is clear that the train system is composed of the multiple units and the spring–dampers system. Intuitively, the overall system can be seen as an interconnection of the two subsystems. The transfer function in (11) can be expressed as

$$\begin{aligned} G(s) &= [M(s) - T(s)\mathcal{L}_{t_n}]^{-1} \\ &= M(s)^{-1}[I_n - T(s)\mathcal{L}_{t_n}M(s)^{-1}]^{-1} \end{aligned} \tag{13}$$

where $M(s)^{-1}$ can be seen as the transfer function of the units system and $T(s)\mathcal{L}_{t_n}$ can be seen as the transfer function of the spring–dampers system coupling the units. If we define a transfer function $S_1 = \begin{bmatrix} 0 & I_n \\ I_n & T(s)\mathcal{L}_{t_n} \end{bmatrix} \in \mathbb{C}_{2n\times 2n}$ and a transfer function $S_2 = M(s)^{-1} = \text{diag}\{\frac{1}{m_i s^2}\} \in \mathbb{C}_{n\times n}$, the transfer function $G(s)$ above can be constructed in the form of the Redheffer Star product $S_1 \star S_2 = G(s)$ in Lemma 2.1. The star product is utilized to describe the relationships of interconnected systems. According to Lemma 2.1, the NI properties of the interconnected system will be preserved if both S_1 and S_2 are NI. It is obvious that the units systems $M(s)^{-1} = S_2$ consisting of multiple double integrator systems is NI according to the Definition 2.1. Since the matrix $j(S_1(j\omega) - S_1(j\omega)^*)$ of transfer function $S_1(s)$ is $\begin{bmatrix} 0_{n\times n} & 0_{n\times n} \\ 0_{n\times n} & k\mathcal{L}_{t_n} \end{bmatrix} \geq 0$, S_1 is also NI according to Definition 2.1. Therefore, the train system with multiple units interconnected by spring–damper systems is NI.

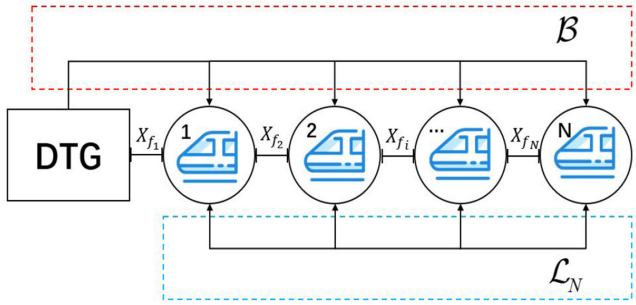

Fig. 2. Networked train platoon model considering the information topology.

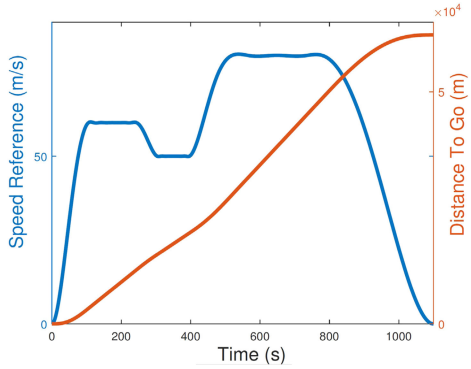

Fig. 3. Speed profile and distance-to-go (DTG) curve for the train platoons.

It is worth mentioning that the locomotive-hauled trains, which are usually modeled as point-mass systems, are also NI because their transfer functions $1/ms^2$ are double-integrator systems, allowing the implementation of our control schemes.

C. Controller Objectives

First, the model of a train platoon is clarified as shown in Fig. 2. There are totally N trains in the platoon, and the communication graph is assumed to be undirected and connected, which is described by a Laplacian matrix $\mathcal{L}_N$. The position of the train platoon is determined by a (DTG curve calculated by the control center, which serves as a motion reference trajectory for the platoon to follow. The connection relationships of the trains to the DTG curve are described by a matrix $\mathcal{B} = \text{diag}_{i=1}^{N}\{b_i\}$ where $b_i = 1$ indicates having access to [19].

To avoid collision, all following trains in the platoon should operate in a prescribed formation. Inspired by the cooperative tracking scheme for solving the rendezvous problem in [9], a distance offset vector $\boldsymbol{X}_f$ is introduced for formation tracking

$$\boldsymbol{X}_f = [\boldsymbol{X}_{f_1}^T, \ldots, \boldsymbol{X}_{f_N}^T]^T \tag{14}$$

where the interval distances in Fig. 2 are included. Each train in the platoon should track the motion reference defined as $(\boldsymbol{d}_{\text{go}} + \boldsymbol{X}_{fi})$ $\forall i \in \{1, 2, \ldots, N\}$, which is the addition of the DTG vector $\boldsymbol{d}_{\text{go}}$ and the offset vector $\boldsymbol{X}_{fi}$. The DTG used in this work is illustrated in Fig. 3. The train i is supposed to converge to $(\boldsymbol{d}_{\text{go}} + \boldsymbol{X}_{fi})$ by the proposed controllers.

The proposed controllers are supposed to be robust to various disturbances $\mathfrak{L}_2[0,\infty]$, which include the resistance disturbances w_1 to the driving forces and w_2 to the position outputs. The disturbances w_1 are composed of two parts w_{1_a} and w_{1_s}. The first part $w_{1_a} = a + bv + cv^2$ is the basic aerodynamic resistances expressed by the Davis equation in [11] where a, b, and c are empirical constants. The second part is the extra operational resistances modeled as $w_{1_s} = \alpha \sin(\omega t + \beta)$ where α, ω, and β are also empirical coefficients. The output disturbances w_2 caused by uncertainties of the position sensors are also modeled in the same form of w_{1_s}.

Moreover, the International Organization for Standardization (ISO) uses the root-mean-square-error (RMSE) value of vibrational accelerations to evaluate the effect of vibration on ride comfort [20]. Therefore, the RMSE of the longitudinal vibrational acceleration of unit i in train j is defined as follows to evaluate the improvement on the ride comfort:

$$a_{v_{ij}} = \left\{ \frac{1}{\tau} \int_{t_0}^{t_0+\tau} [a_{x_{ij}}(t)]^2 dt \right\}^{\frac{1}{2}} \tag{15}$$

where $a_{x_{ij}} = a_{u_{ij}} - a_{\mathrm{DTG}}$ is the acceleration error between the acceleration $a_{u_{ij}}$ of the unit i in the train j and the acceleration reference a_{DTG} calculated from the DTG curve.

In summary, the objectives of the proposed controller can be listed as follows.

1) Each train realizes robust tracking of the predefined DTG in a prescribed formation under external disturbances $w_1, w_2 \in \mathfrak{L}_2[0,\infty]$:

$$(\boldsymbol{y}_i - \boldsymbol{y}_{ss_i}) \to \mathfrak{L}_2[0,\infty] \quad \forall i \in \{1,2,\ldots,N\} \tag{16}$$

where $\boldsymbol{y}_{ss_i} = (\boldsymbol{d}_{\mathrm{go}} + \boldsymbol{X}_{fi})$ is the final convergence trajectory for the ith train.

2) The RMSE of the longitudinal vibrational acceleration of each train defined as follows:

$$a_{T_j} = \frac{1}{n} \sum_{i=1}^{n} a_{v_{ij}} \quad \forall j \in \{1,\ldots,N\} \tag{17}$$

is reduced benefiting from the consensus reached between units, where $a_{v_{ij}}$ is defined in (15) and a_{T_j} is the RMSE value of the jth train in the platoon.

D. Networked Train Platooning Systems

Based on the CBTC system, the exact positions of all the units in an EMU train could be obtained and transmitted between other EMU trains conveniently, so the position output feedback control is implemented. The Laplacian matrix defined as $\mathcal{L}_a = \mathcal{L}_N + \mathcal{B}$ is utilized to describe the information topologies among trains as well as the control station. By virtue of building networked train platooning models, the control problem could be transferred into an internal stability problem, which is clarified as follows for homogeneous and heterogeneous situations, respectively.

1) Homogeneous Train Platooning: First, the platoon composed of N trains of the same model can be regarded as an augmented NI plant composed of multiple NI subsystems

$$\tilde{\boldsymbol{y}} = \tilde{G}(s)\boldsymbol{u} = (I_N \otimes G(s))\boldsymbol{u} \tag{18}$$

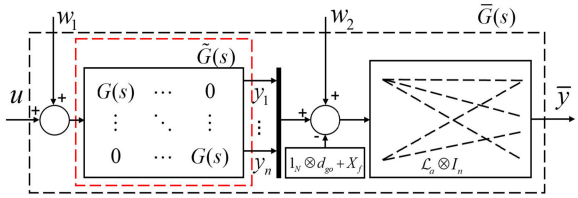

Fig. 4. Overall homogeneous network system.

where $\tilde{\boldsymbol{y}} = [\boldsymbol{y}_1^T, \boldsymbol{y}_2^T, \ldots, \boldsymbol{y}_N^T]^T \in \mathbb{R}_{Nn\times 1}$ denotes the output vector of positions, which could be measured by sensors, $\boldsymbol{u} = [\boldsymbol{u}_1^T, \boldsymbol{u}_2^T, \ldots, \boldsymbol{u}_N^T]^T \in \mathbb{R}_{Nn\times 1}$ denotes the input vector of driving forces, and $G(s)$ is the transfer function of each train.

Suppose that a networked system considering communication topology among trains is constructed as follows:

$$\bar{\boldsymbol{y}} = \bar{G}(s)\boldsymbol{u} = (\mathcal{L}_N \otimes I_n)(I_N \otimes G(s))\boldsymbol{u} = (\mathcal{L}_N \otimes G(s))\boldsymbol{u} \tag{19}$$

where $\bar{\boldsymbol{y}} = [\bar{\boldsymbol{y}}_1^T, \bar{\boldsymbol{y}}_2^T, \ldots, \bar{\boldsymbol{y}}_N^T]^T \in \mathbb{R}_{Nn\times 1}$ denotes the position errors between connected trains and $\boldsymbol{u}$ is the same. The Laplacian matrix $\mathcal{L}_N$ describes the undirected and connected graph. Each train has n units. It can be seen that $\boldsymbol{y}$ reaches consensus when $\bar{\boldsymbol{y}} \to 0$.

To realize reference tracking in a predefined formation, the vectors d_{go} calculated from the control station and X_f defining formation are included in the network platoon model. By utilizing the matrix $\mathcal{L}_a = \mathcal{L}_N + \mathcal{B}$ and subtracting $(\mathbf{1}_N \otimes \boldsymbol{d}_{\mathrm{go}} + \boldsymbol{X}_f)$ from $\boldsymbol{y}$, the network platoon system is constructed as depicted in Fig 4. The position errors vector $\bar{\boldsymbol{y}}$ can be split into two parts according to the null-space property of Laplacian matrix in (1)

$$\begin{aligned} \bar{\boldsymbol{y}} &= (\mathcal{L}_a \otimes I_n)(\boldsymbol{y} - \mathbf{1}_N \otimes \boldsymbol{d}_{\mathrm{go}} - \boldsymbol{X}_f) \\ &= (\mathcal{L}_N \otimes I_n)(\boldsymbol{y} - X_f) + (\mathcal{B} \otimes I_n)(\boldsymbol{y} - \mathbf{1}_N \otimes \boldsymbol{d}_{\mathrm{go}} - \boldsymbol{X}_f). \end{aligned} \tag{20}$$

It can be seen that the first term denotes the position errors of connected trains within the platoon, whereas the second term denotes the relative position errors between trains and the motion reference. The objective in (16) could be realized if a robust controller drives $\bar{\boldsymbol{y}} \to 0$. According to [10, Lemma 3], the augmented system is also an NI system.

2) Heterogeneous Train Platooning: For heterogeneous scenarios, the overall networked system $(\mathcal{L}_a \otimes I_n) \cdot \mathrm{diag}_{i=1}^{N}\{G_i(s)\}$ is not NI anymore due to asymmetry even through each train model $G_i(s)$ is NI. To solve this, we utilize the incidence matrix calculated by $\mathcal{L}_a = \mathcal{Q}_a \mathcal{Q}_a^T$ from the Laplacian matrix.

The transfer function $\hat{G}_i(s)$ with dimension $n_i \times n_i$ is assumed to have access to the motion reference. In order to deal with consensus of outputs with different dimensions, $\hat{G}_i(s)$ should be padded to the maximum dimension $n_{\max} = \max_{i=1}^{N}\{n_i\}$ if $n_i \le n_{\max}$ according to [9]

$$\begin{aligned} G_i(s) &= \begin{bmatrix} \hat{G}_i(s)_{n\times n} & \mathbf{0}_{n\times\Delta n} \\ \mathbf{0}_{\Delta n\times n} & \boldsymbol{d}_{\Delta n\times\Delta n} \end{bmatrix} \\ \boldsymbol{u}_i(s) &= \begin{bmatrix} \hat{\boldsymbol{u}}_i^T|_{n\times 1} \\ \boldsymbol{d}_{\Delta n\times 1} \end{bmatrix} \boldsymbol{y}_i(s) = \begin{bmatrix} \hat{\boldsymbol{y}}_i^T|_{n\times 1} \\ \boldsymbol{d}_{\Delta n\times 1} \end{bmatrix} \end{aligned} \tag{21}$$

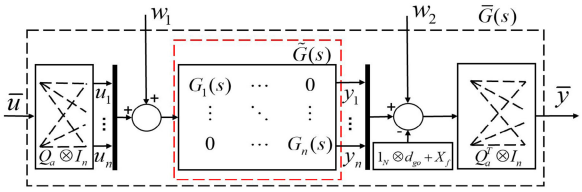

Fig. 5. Overall heterogeneous network system.

where $\Delta n = n_{\max} - n_i$ and $\boldsymbol{d}$ is the DTG curve. The output vector $\bar{\boldsymbol{y}}$ of the overall system in Fig. 5 is derived

$$\begin{aligned}\bar{\boldsymbol{y}} &= (\mathcal{Q}_a \otimes I_n)(\boldsymbol{y} - 1 \otimes \boldsymbol{d}_{do} - \boldsymbol{X}_f) \\ &= \begin{bmatrix}\mathcal{Q}^T \\ \mathcal{Q}_b^T\end{bmatrix} \otimes I_n(\boldsymbol{y} - \mathbf{1}_N \otimes \boldsymbol{d}_{\text{go}} - \boldsymbol{X}_f) \\ &= \begin{bmatrix}(\mathcal{Q}^T \otimes I_n)(\boldsymbol{y} - \boldsymbol{X}_f) \\ (\mathcal{Q}_b^T \otimes I_n)(\boldsymbol{y} - \mathbf{1}_N \otimes \boldsymbol{d}_{\text{go}} - \boldsymbol{X}_f)\end{bmatrix}\end{aligned} \tag{22}$$

where the incidence matrix $\mathcal{Q}$ is from $\mathcal{L}_N = \mathcal{Q}\mathcal{Q}^T$ and $\mathcal{Q}_b$ is from $\mathcal{B} = \mathcal{Q}_b\mathcal{Q}_b^T$, $\bar{\boldsymbol{y}} = [\bar{\boldsymbol{y}}_1^T, \bar{\boldsymbol{y}}_2^T, \ldots, \bar{\boldsymbol{y}}_{l+1}^T]^T \in \mathbb{R}_{(l+1)n_{\max}\times 1}$. Similar to the homogeneous situation, the heterogeneous platoon follows the DTG curve in formation determined by $\boldsymbol{X}_f$ if the output $\bar{\boldsymbol{y}}$ converges to zero. According to [9, Lemma 4], the system $(Q_a^T \otimes I_n)\tilde{G}(s)(Q_a \otimes I_n)$ is still NI.

IV. Formation Control for Homogeneous Train Platoons

The controller designed for homogeneous train platoons along with corresponding simulation results are presented in this section. A homogeneous train platoon is a platoon, which is composed of multiple trains of the same model. To be more specific, the power configuration and the number of units of all the trains are the same, whereas the mass of each train can be different.

For a networked homogeneous platoon model in Fig 4, it can be seen that the platoon tracks the DTG curve in a prescribed formation specified by $\boldsymbol{X}_f$ when $\bar{\boldsymbol{y}}$ in (20) converges to zero. By virtue of stability theories of NI systems in Lemma 2.2, a robust SNI controller is proposed to stabilize the interconnected system under disturbances $\omega_1, \omega_2 \in \mathfrak{L}_2 \in [0, \infty]$.

A. Controller Design

Since the mass of each train is changing during operation, the stability conditions associated with it should be verified theoretically each time. To avoid frequent verification, the fully loaded scenario is considered when designing the controller, and the stability conditions are still satisfied as proved in the following. Assuming each train is fully loaded, the transfer function matrix of the networked platoon system is

$$\bar{G}_x(s) = (\mathcal{L}_a \otimes G_x(s)) \tag{23}$$

where $G_x(s)$ denotes the transfer function matrix of a fully loaded train as described in (10). The controller is capable of handling the general conditions where the mass of each train is uncertain.

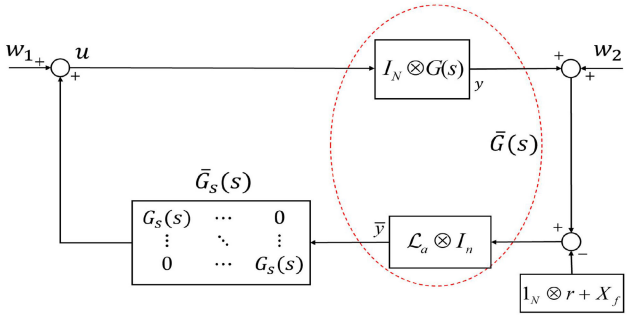

Fig. 6. Formation control structure for homogeneous train platoons.

Theorem 4.1: Consider a train platoon consisting of N trains with the same model. Each train is described by (11) and communicates through an undirected and connected graph. The matrix $\mathcal{B}$ models the communicating connection to the external reference. Given any SNI control law $G_s(s)$, robust formation control can be achieved for the networked train platoon system via the following control law:

$$\begin{aligned}\boldsymbol{u} &= ((\mathcal{L}_N + \mathcal{B}) \otimes G_s(s))\boldsymbol{e} \\ \boldsymbol{e} &= \boldsymbol{y} - (\mathbf{1}_N \otimes \boldsymbol{d}_{\text{go}}) - \boldsymbol{X}_f\end{aligned} \tag{24}$$

as shown in Fig. 6 or in a distributed manner for each train i

$$\begin{aligned}\boldsymbol{u}_i = G_s(s)\Big(\sum_{j=1}^{N} a_{ij}((\boldsymbol{y}_i - \boldsymbol{X}_{f_i}) - (\boldsymbol{y}_j - \boldsymbol{X}_{f_j})) \\ + \boldsymbol{b}_i(\boldsymbol{y}_i - \boldsymbol{d}_{\text{go}} - \boldsymbol{X}_{f_i})\Big)\end{aligned} \tag{25}$$

if the interconnection system $[\bar{G}_x(s), \bar{G}_s(s)]$ of the networked platoon system in (23) and the SNI controller $\bar{G}_s(s) = I_N \otimes G_s(s)$ satisfies the conditions (4) and either (5) or (6) in Lemma 2.2. The coefficient a_{ij} is the elements of the adjacency matrix and b_j denotes the element of the matrix $\mathcal{B}$.

Proof: The constant matrices $\bar{G}_{2_x}, \bar{G}_{0_x}$, and $\bar{G}_{2_x}$ of the networked system $\bar{G}_x(s)$ are calculated via (2) and $\bar{J}_x$ satisfies $\bar{G}_{2_x} = \bar{J}_x\bar{J}_x^T$. The matrix $\bar{N}_{2_x}$ is calculated by substituting $\bar{J}_x$ and the dc gain of the controller $\bar{G}_s(0)$ into (3). All the matrices before correspond to the fully loaded situation. Since $\bar{G}_{1_x} = \mathcal{L}_a \otimes G_{1_x} = \mathbf{0}$ according to (12), the overall system $[\bar{G}_x(s), \bar{G}_s(s)]$ is internally stable according to Lemma 2.2.

For the general cases where the mass of each train could be different, the coefficient matrix of the augmented system $\bar{G}_2$ corresponding the general transfer function $\bar{G}(s)$ can be derived

$$\begin{aligned}\bar{G}_2 &= (\mathcal{L}_a \otimes I_n)(I_N \otimes G_2) \\ &= (\mathcal{L}_a \otimes I_n)(\mathcal{D}_N \otimes G_{2_x}) = \mathcal{L}_a\mathcal{D}_N \otimes G_{2_x} \\ &= ((J_aJ_d)(J_aJ_d)^T) \otimes (J_xJ_x^T) \\ &= ((J_aJ_d) \otimes J_x)((J_aJ_d) \otimes J_x)^T\end{aligned} \tag{26}$$

where $\mathcal{L}_a = \mathcal{L}_N + \mathcal{D} = J_aJ_a^T$ and $\mathcal{D}_N = \text{diag}_{i=1}^N\{\frac{1}{d_i}\} = J_dJ_d^T$ describes the changing coefficients of the mass for each train in the platoon. Therefore, the decomposed matrix of $\bar{G}_2$ is

$$\bar{J} = (J_aJ_d) \otimes J_x \cdot 1 = (J_a \otimes J_x)J_d = \bar{J}_xJ_d. \tag{27}$$

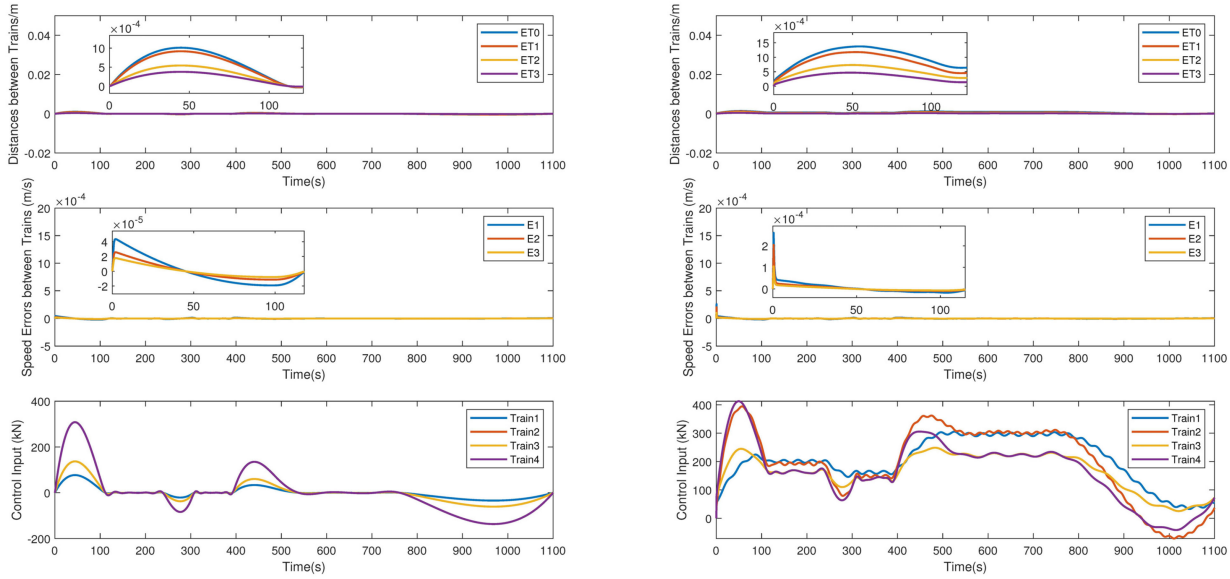

(a) (b)

Fig. 7. Robust formation tracking results. (a) Position errors, speed errors. and control inputs of trains without disturbances. (b) Position errors, speed errors, and control inputs of trains under disturbances.

Since the condition in (4) is satisfied for $\bar{J}_x$, the condition for $\bar{J}$ can also be satisfied: $\bar{J}_x^T G_s(0)\bar{J}_x < 0 \Rightarrow \bar{J}^T G_s(0)\bar{J} = J_d^T(\bar{J}_x^T G_s(0)\bar{J}_x)J_d < 0$. Then, the matrix $\bar{N}_2$ defined in (3) is calculated to check the other stability condition

$$\begin{aligned}\bar{N}_2 &= \bar{G}_s(0) - \bar{G}_s(0)\bar{J}(\bar{J}^T\bar{G}_s(0)\bar{J})^{-1}\bar{J}^T\bar{G}_s(0)\\ &= \bar{G}_s(0)\\ &\quad - \bar{G}_s(0)(\bar{J}_x\bar{J}_d)(\bar{J}_d\bar{J}_x^T\bar{G}_s(0)\bar{J}_x\bar{J}_d)^{-1}(\bar{J}_x\bar{J}_d)^T\bar{G}_s(0)\\ &= \bar{G}_s(0) - \bar{G}_s(0)\bar{J}_x(\bar{J}_x^T\bar{G}_s(0)\bar{J}_x)^{-1}\bar{J}_x^T\bar{G}_s(0) = \bar{N}_{2_x}\end{aligned} \tag{28}$$

which indicates that the matrix $\bar{N}_2$ remains constant regardless of the changing mass of each train. According to (12), the matrix $\bar{G}_0 = \mathcal{L}_a \otimes G_0 = \mathcal{L}_a \otimes G_{0_x} = \bar{G}_{0_x}$, so the conditions (5) or (6) are also satisfied when the mass of each train is changing. Therefore, the overall system in Fig. 6 is internally stable as guaranteed by Lemma 2.2, indicating the third objective of the controller is reached.

The stability of the overall system drives the outputs $\bar{\boldsymbol{y}}$ in (19) to converge to $\mathbf{0}$. The term $(\mathcal{L}_N \otimes I_n)(\boldsymbol{y} - \boldsymbol{X}_f) \to \mathbf{0}$ implies that the relative outputs for the agents eventually converge to the formation vector. The other term $(\mathcal{B} \otimes I_n)(\boldsymbol{y} - \mathbf{1}_N \otimes \boldsymbol{d}_{\text{go}} - \boldsymbol{X}_f) \to \mathbf{0}$ implies that the outputs of the trains connecting to the reference finally converge to the prescribed reference.

Since the position of each unit in a train is coordinated via the proposed controller, the consensus is realized not only among trains, but also among units, which is beneficial to reduce the RMSE of longitudinal vibration acceleration defined in (17) of the second objective. Moreover, since the above controller is based on the position feedback consensus, the synchronization of the velocities of trains in the platoon can be realized. Compared with the traditional fixed-block signaling (FBS) system where the following train can only depart after the preceding train leaves the front block, the train can depart simultaneously using our controller. Therefore, the departure headway $\mathcal{T}_d$ defined as follows could be reduced:

$$\mathcal{T}_d = \mathcal{T}_N - \mathcal{T}_1 \tag{29}$$

where $\mathcal{T}_1$ and $\mathcal{T}_N$ denote the time when the heading and the last train arrives at the station, respectively.

B. Simulation Results for Homogeneous Platoons

To verify the effectiveness of the proposed scheme, the simulation of multiple homogeneous trains is presented in this section. The parameterization of the simulation is based on the China Railway CRH3C train, which is composed of four units. The platoon is composed of four CRH3C trains, and they are virtually connected one by one through communication. The interval distance between trains in the formation is set to be 500 m, which corresponds a formation vector of $[0,\ 500,\ 1000,\ 1500]^T \otimes \mathbf{1}_{4\times 1}$. The leading train obtains DTG information in real time, and hence, $\mathcal{B} = \text{diag}\{1, 0, 0, 0\}$.

Referring to the drag coefficients in [11], we set the operational resistance forces (in newton) of the four trains as $144\,000 + 1920v_1 + 76.8v_1^2$, $48\,000 + 600v_2 + 48v_2^2$, $96\,000 + 600v_3 + 24v_3^2$, $153\,600 + 1200v_4 + 96v_4^2$. Besides the resistance, the operation disturbances including forces brought by tunnel, curve, slope, etc., are also considered in the simulation. Disturbance forces (in newton) to the input are $7200\sin(0.2t)$, $2400\sin(0.3t)$, $3600\sin(0.1t)$, and $2160\sin(0.35t)$, respectively, while disturbances applied to the system outputs of the four trains are defined as $0.05\sin(0.1t)$, $0.1\sin(0.2t)$, $0.08\sin(0.4t)$, and $0.12\sin(0.3t)$. The mass-changing coefficients matrix in (26) is defined as $\mathcal{D}_N = \text{diag}\{0.85, 0.9, 0.95, 0.8\}$.

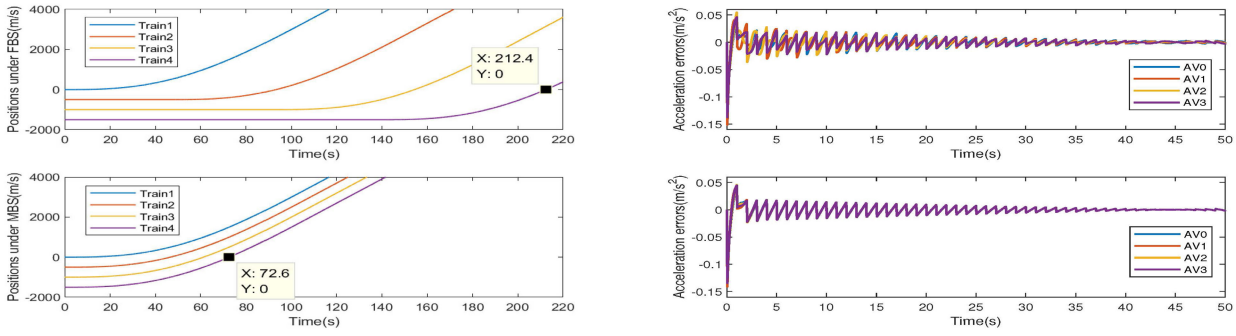

(a) (b)

Fig. 8. Improvement in line efficiency and ride comfort. (a) Position trajectories under FBS (upper) and by proposed controller (lower). (b) Acceleration errors comparison.

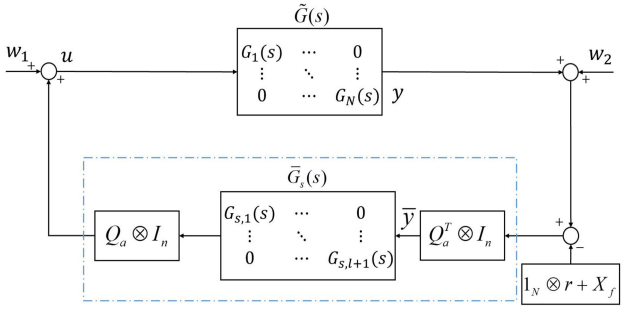

Fig. 9. Formation control structure for heterogeneous train platoons.

The SNI tracking controller for the platoon with four trains is chosen as $G_s(s) = 2 \times 10^7 \cdot \text{diag}_{i=1}^4 (\frac{-30s-78}{3s+570})$. To demonstrate the formation control performance of the proposed method in Theorem 4.1, the results of tracking experiments are presented in Fig. 7. The distance error here is defined as $\mathbf{ET}_i = \boldsymbol{y}_i - (\boldsymbol{d}_{\text{go}} + \boldsymbol{X}_{f_i})$ for the train i, which denotes the error between the real-time position $\boldsymbol{y}_i$ and the motion reference $\boldsymbol{d}_{\text{go}} + \boldsymbol{X}_{f_i}$. To demonstrate the robustness of the proposed controller, both the results without disturbances in (a) and results under disturbances in (b) are presented. It is found that the speed and distance errors converge to zero throughout the duration and the controller works effectively even under disturbances.

The results of $\mathcal{T}_d$ under both MBS and FBS are presented in Fig. 8(a). There is an apparent reduction on the departure time (212.4 s versus 72.6 s) by the proposed controller, which illustrates a better line utilization efficiency. The error between the acceleration of the unit and the acceleration reference is used to represent the longitudinal vibration. To demonstrate the improvement on ride comfort, the errors of the four units in the heading train are presented in Fig 8(b). The upper figure shows the errors when the control input is averagely applied to the four units, whereas the figure below presents the results using the proposed controller. The a_T values defined in (17) of the four trains are 0.0066, 0.0074, 0.0071, 0.0071 (m/s^2), respectively, in the first case, whereas the values are 0.0065, 0.0069, 0.0066, 0.0068 (m/s^2), respectively, in the second case. The reduction implies that ride comfort is improved.

V. Formation Control for Heterogeneous Train Platoons

A controller for heterogeneous train platoons along with the corresponding simulation results are presented in this section. A heterogeneous train platoon implies that the platoon is composed of multiple trains of different model. For a networked heterogeneous platoon model in Fig 5, a robust SNI controller is proposed to stabilize the interconnected system under disturbances $\omega_1, \omega_2 \in \mathfrak{L}_2 \in [0, \infty]$.

A. Controller Design

Similar to the homogeneous scenario, the fully loaded situation is considered for robustness to mass uncertainty. The train platoon with possibly maximum mass is

$$\tilde{G}_x(s) = \underset{i=1}{\overset{N}{\text{diag}}}\{G_{x_i}(s)\} \tag{30}$$

where $G_{x_i}(s)$ has been properly padded via (21). Construct the transfer function $\bar{G}_x(s) = (\mathcal{Q}_a^T \otimes I_n)\tilde{G}_x(s)(\mathcal{Q}_a \otimes I_n)$ of the networked heterogeneous platoon system considering the communication topology via (22). The control law for heterogeneous train platoons is proposed in the following.

Theorem 5.1:

Consider a train platoon consisting of N heterogeneous trains. Each train is described by (11) and communicates through an undirected and connected graph. Define the controller $\bar{G}_s(s) = \text{diag}_{k=1}^l\{G_{s,k}(s)\}$. Robust formation control can be achieved for the train platoon system in Fig. 9 via the following control law:

$$\begin{aligned} \boldsymbol{u} &= ((\mathcal{Q}_a \otimes I_n)\bar{G}_s(s)(\mathcal{Q}_a^T \otimes I_n))\boldsymbol{e} \\ \boldsymbol{e} &= \boldsymbol{y} - (\mathbf{1}_N \otimes \boldsymbol{d}_{\text{go}}) - \mathbf{X}_f \end{aligned} \tag{31}$$

or in a distributed manner for each train i

$$\begin{aligned} \boldsymbol{u}_i = (\sum_{j=1}^{N} a_{ij} G_{s,k}(s)((\boldsymbol{y}_i - \boldsymbol{X}_{f_i}) - (\boldsymbol{y}_j - \boldsymbol{X}_{f_j})) \\ + b_i G_{s,k}(s)(\boldsymbol{y}_i - \boldsymbol{d}_{go_i} - \boldsymbol{X}_{f_i})) \end{aligned} \tag{32}$$

if the interconnection system $[\bar{G}_x(s), \bar{G}_s(s)]$ of the overall fully loaded platoon system satisfies the conditions (4) and either (5)

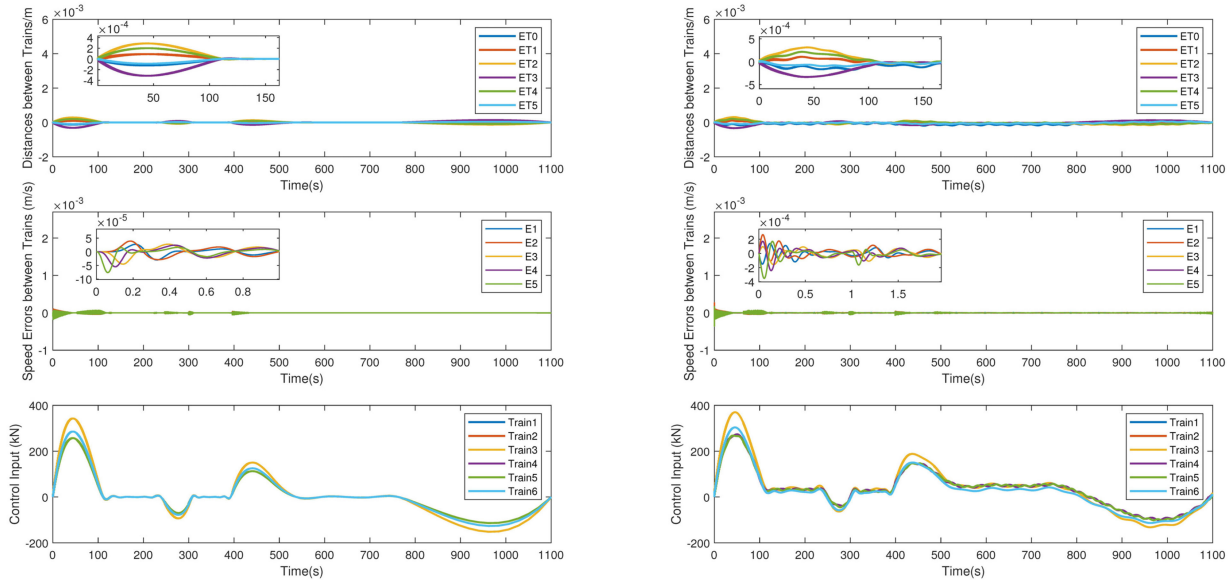

(a) (b)

Fig. 10. Robust formation tracking results. (a) Position errors, speed errors, and control inputs of trains without disturbances. (b) Position errors, speed errors, and control inputs of trains under disturbances.

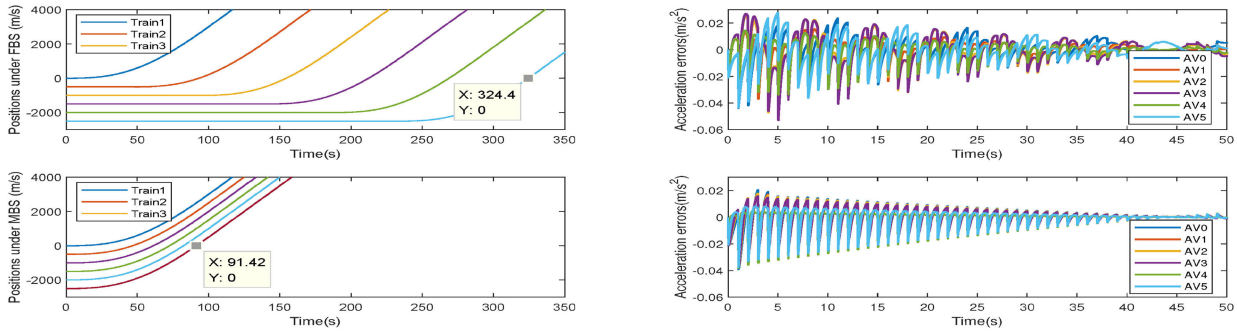

(a) (b)

Fig. 11. Improvement in line efficiency and ride comfort. (a) Position trajectories under FBS (upper) and by proposed controller (lower). (b) Acceleration trajectories and acceleration errors.

or (6) in Lemma 2.2. The number $k \in \{1, \ldots, l\}$ is the edge-connected vertex i and j, and $k_b \in \{1, \ldots, l_b\}$ corresponds to the link number connecting the reference $(\boldsymbol{d}_{\text{go}} + \boldsymbol{X}_{f_i})$ to the train i.

Proof: The overall system $[\bar{G}_x(s), \bar{G}_s(s)]$ is internally stable according to Lemma 2.2. Similar to the process in the homogeneous case, the stability of the overall system is analyzed first. Similar to (27), the decomposed matrix of the system's constant matrix $\bar{G}_2$ is $\bar{J} = \bar{J}_x J_d$, where $\bar{J}_x$ is calculated from $\bar{G}_{2_x} = \bar{J}_x \bar{J}_x^T$ and J_d is calculated from $\mathcal{D}_N = J_d J_d^T$. The matrix $\bar{G}_{2_x}$ corresponds to the case where all trains are in their maximum mass. The rest proof is the same as the homogeneous situation, which means the effect of the changing mass will not change the stability conditions.

The stability of the overall system drives the system outputs $\bar{\boldsymbol{y}}$ in (22) to converge to $\mathbf{0}$, which leads to $(\mathcal{Q}^T \otimes I_n)(\boldsymbol{y} - \boldsymbol{X}_f) \to \mathbf{0}$ (i.e., the relative outputs among the agents eventually converge to the formation vector) and $(\mathcal{Q}_b^T \otimes I_n)(\boldsymbol{y} - \mathbf{1}_N \otimes \boldsymbol{d}_{\text{go}} - \boldsymbol{X}_f) \to \mathbf{0}$ (i.e., the outputs of the agents connecting to the reference converge to the prescribed reference). Therefore, the objective of tracking is realized. ■

Similar to the homogeneous scenario, the RMSE of longitudinal acceleration as well as departure headway defined in (29) could be reduced via the proposed controller.

B. Simulation Results for Heterogeneous Platoons

The simulation of multiple heterogeneous trains is presented in this section. Besides the CRH3C, other trains in the platoon are assumed to be CRH2A, which has totally six units. Suppose that the platoon contains six trains. The first, second, fourth, and fifth trains are CRH3C, whereas the rest two are CRH2A. The safety interval between the three trains is set to be 500 m. Each train in the platoon has access to the information of neighboring trains and the reference information.

We set the operational resistance forces of the three trains as $108\,000 + 1440v_1 + 57.6v_1^2$, $72\,000 + 900v_2 + 72v_2^2$, $144\,000 + 900v_3 + 36v_3^2$, $108\,000 + 1440v_1 +$

$57.6v_1^2$, $72\,000 + 900v_2 + 72v_2^2$, $144\,000 + 900v_3 + 36v_3^2$ Besides the resistance, the operation disturbances to the input are set to $5400\sin(0.2t)$, $3600\sin(0.3t)$, $5400\sin(0.1t)$ $5400\sin(0.2t)$, $3600\sin(0.3t)$, and $5400\sin(0.1t)$ respectively, whereas disturbances applied to the system outputs of the six trains are defined as $0.05\sin(0.1t)$, $0.1\sin(0.2t)$, $0.08\sin(0.4t)$, $0.05\sin(0.1t)$, $0.1\sin(0.2t)$, and $0.08\sin(0.4t)$. The mass-variation coefficients matrix in (26) is defined as $\mathcal{D}_N = \text{diag}\{0.85, 0.9, 0.95, 0.85, 0.9, 0.95\}$ for the six trains in the platoon.

The SNI tracking controller for the platoon with three trains is chosen as $\bar{G}_s(s) = 5 \times 10^7 \cdot \text{diag}_{i=1}^{6}(\frac{-5s-500}{1s+572})$. The results of tracking experiments are presented in Fig. 10. Both the results without disturbances in (a) and results under disturbances in (b) are presented. It is found that the speed and distance errors converge to a zero throughout the duration and the controller works effectively even under disturbances.

In Fig. 10, the departure headway $\mathcal{T}_d$ for the proposed controller is reduced from 324.4 to 91.4 s, which demonstrates an improvement on line efficiency. As for the improvement on comfort, take the sixth train for instance, the acceleration errors of the six units of it are presented in Fig 11(b) when equally applying the input and using the proposed scheme, respectively. The RMSE values of the six trains defined in (17) are 0.0084, 0.0070, 0.0106, 0.0112 0.0059, 0.0092 (m/s^2), respectively, when the control input is averagely applied to all the units, whereas the values are 0.0080, 0.0070, 0.0065, 0.0061 0.0053, 0.0054 (m/s^2), respectively, via the proposed controller. The reduction illustrates a better ride comfort using the proposed scheme.

VI. Conclusion

In this article, train systems have been modeled as NI systems, and NI theories have been implemented for the cooperative control of train platoons. The NI property of trains considering the physical couplers between units has been analyzed. The homogeneous and heterogeneous train platoons have been constructed as networked NI systems via graph theory. To achieve the controllers' objectives, the control schemes have been proposed using the relative NI stability theories. The controllers are robust to mass variation, which has been rigorously proved. Via comparing the position and speed errors with and without disturbances, simulation experiments have been presented to illustrate the robustness to external disturbances. Moreover, the improvements on line efficiency and ride comfort via the proposed controllers have been demonstrated. In the future, the model uncertainties of trains will be further studied.

References

[1] R. D. Pascoe and T. N. Eichorn, "What is communication-based train control?" *IEEE Veh. Technol. Mag.*, vol. 4, no. 4, pp. 16–21, Dec. 2009.

[2] B. Bu, F. R. Yu, and T. Tang, "Performance improved methods for communication-based train control systems with random packet drops," *IEEE Trans. Intell. Transp. Syst.*, vol. 15, no. 3, pp. 1179–1192, Jun. 2014.

[3] S. Gordon and D. Lehrer, "Coordinated train control and energy management control strategies," in *Proc. ASME/IEEE Joint Railroad Conf.*, 1998, pp. 165–176.

[4] S. Su, T. Tang, C. Roberts, and L. Huang, "Cooperative train control for energy-saving," in *Proc. IEEE Int. Conf. Intell. Rail Transp.*, 2013, pp. 7–12.

[5] A. Lanzon and I. R. Petersen, "Stability robustness of a feedback interconnection of systems with negative imaginary frequency response," *IEEE Trans. Autom. Control*, vol. 53, no. 4, pp. 1042–1046, May 2008.

[6] M. A. Mabrok, A. G. Kallapur, I. R. Petersen, and A. Lanzon, "Generalizing negative imaginary systems theory to include free body dynamics: Control of highly resonant structures with free body motion," *IEEE Trans. Autom. Control*, vol. 59, no. 10, pp. 2692–2707, Oct. 2014.

[7] A. Ferrante and L. Ntogramatzidis, "Some new results in the theory of negative imaginary systems with symmetric transfer matrix function," *Automatica*, vol. 49, no. 7, pp. 2138–2144, 2013.

[8] C. Cai and G. Hagen, "Stability analysis for a string of coupled stable subsystems with negative imaginary frequency response," *IEEE Trans. Autom. Control*, vol. 55, no. 8, pp. 1958–1963, Aug. 2010.

[9] J. Wang, A. Lanzon, and I. R. Petersen, "Robust cooperative control of multiple heterogeneous negative-imaginary systems," *Automatica*, vol. 61, pp. 64–72, 2015.

[10] J. Wang, A. Lanzon, and I. Petersen, "Robust output feedback consensus for networked negative-imaginary systems," *IEEE Trans. Autom. Control*, vol. 60, no. 9, pp. 2547–2552, Sep. 2015.

[11] H. Dong, S. Gao, and B. Ning, "Cooperative control synthesis and stability analysis of multiple trains under moving signaling systems," *IEEE Trans. Intell. Transp. Syst.*, vol. 17, no. 10, pp. 2730–2738, Oct. 2016.

[12] S. Gao, H. Dong, B. Ning, and Q. Zhang, "Cooperative prescribed performance tracking control for multiple high-speed trains in moving block signaling system," *IEEE Trans. Intell. Transp. Syst.*, vol. 20, no. 7, pp. 2740–2749, Jul. 2019.

[13] J. Félez, Y. Kim, and F. Borrelli, "A model predictive control approach for virtual coupling in railways," *IEEE Trans. Intell. Transp. Syst.*, vol. 20, no. 7, pp. 2728–2739, Jul. 2019.

[14] Q. Song and Y.-D. Song, "Data-based fault-tolerant control of high-speed trains with traction/braking notch nonlinearities and actuator failures," *IEEE Trans. Neural Netw.*, vol. 22, no. 12, pp. 2250–2261, Dec. 2011.

[15] Y. Wang, Y. Song, H. Gao, and F. L. Lewis, "Distributed fault-tolerant control of virtually and physically interconnected systems with application to high-speed trains under traction/braking failures," *IEEE Trans. Intell. Transp. Syst.*, vol. 17, no. 2, pp. 535–545, Feb. 2016.

[16] X. Wang, S. Li, T. Tang, X. Wang, and J. Xun, "Intelligent operation of heavy haul train with data imbalance: A machine learning method," *Knowl. Based Syst.*, vol. 163, pp. 36–50, 2019.

[17] G. Liu and Z. Hou, "Cooperative adaptive iterative learning fault-tolerant control scheme for multiple subway trains," *IEEE Trans. Cybern.*, pp. 1–14, to be published, doi: 10.1109/TCYB.2020.2986006

[18] A. Ferrante, A. Lanzon, and L. Ntogramatzidis, "Foundations of not necessarily rational negative imaginary systems theory: Relations between classes of negative imaginary and positive real systems," *IEEE Trans. Autom. Control*, vol. 61, no. 10, pp. 3052–3057, Oct. 2016.

[19] W. Ni and D. Cheng, "Leader-following consensus of multi-agent systems under fixed and switching topologies," *Syst. Control Lett.*, vol. 59, no. 3/4, pp. 209–217, 2010.

[20] *Mechanical Vibration and Shock-Evaluation of Human Exposure to Whole-Body Vibration—Part 1: General requirements*, ISO 2631-1:1997, ISO, Geneva, Switzerland, 1997.

Chunyu Li received the B.S. degree in vehicle engineering from Hunan University, Changsha, China, in 2015, and the M.S. degree in vehicle engineering from the University of Bath, Bath, U.K., in 2016. He is currently working toward the Ph.D. degree in aerospace engineering with the Beijing Institute of Technology, Beijing, China.

His current research interests include cooperative control and state estimation for aerial vehicles.

Jianan Wang (Senior Member, IEEE) received the B.S. degree in control theory and engineering from Beijing Jiaotong University, Beijing, China, in 2004, the M.S. degree in control theory and engineering from the Beijing Institute of Technology, Beijing, in 2007, and the Ph.D. degree in aerospace engineering from Mississippi State University, Starkville, MS, USA, in 2011.

He is currently an Associate Professor with the School of Aerospace Engineering, Beijing Institute of Technology. His research interests include cooperative control of multiple dynamic systems, UAV formation control, cooperative guidance, and estimation of sensor networks.

Dr. Wang is a Senior Member of AIAA.

Jiayuan Shan received the B.S. degree in mechanical engineering from Huazhong University of Science and Technology, Wuhan, China, in 1988, the M.S. degree in aerospace engineering and Ph.D. degree in control engineering from the Beijing Institute of Technology, Beijing, China, in 1991 and 1999, respectively.

He is currently a Professor with the School of Aerospace Engineering, Beijing Institute of Technology. He is also the Principal Professor in the direction of flight dynamics and control. His research interests include guidance, navigation, and control of the aircraft and hardware-in-the-loop simulation.

Alexander Lanzon received the B.Eng. (Hons). degree in electrical and electronic engineering from the University of Malta, Msida, Malta, in 1995, and the M.Phil. degree in robot control and the Ph.D. degree in control engineering from the University of Cambridge, Cambridge, U.K., in 1997 and 2000, respectively.

He has held research and academic positions with the Georgia Institute of Technology, Atlanta, GA, USA, and the Australian National University, Canberra, ACT, Australia, and industrial positions with ST-Microelectronics, Ltd., Kirkop, Malta; Yaskawa Denki (Tokyo), Ltd., Saitama-Ken, Japan; and National ICT Australia, Ltd., Canberra. In 2006, he joined the University of Manchester, Manchester, U.K., where he is currently the Chair in control engineering. His research interests include the fundamentals of feedback control theory, negative imaginary systems theory, $\mathcal{H}_\infty$ control theory, robust linear and nonlinear feedback control systems, and applying robust control theory to innovative mechatronics, robotics, and drone applications.

Prof. Lanzon is a Fellow of the Institute of Mathematics and Its Applications, the Institute of Measurement and Control, and the Institution of Engineering and Technology. He was an Associate Editor for the IEEE TRANSACTIONS ON AUTOMATIC CONTROL from 2012 to 2018, and as a Subject Editor of the *International Journal of Robust and Nonlinear Control* from 2012 to 2015.

Ian R. Petersen (Fellow, IEEE) was born in Victoria, Australia. He received the Ph.D. degree in electrical engineering from the University of Rochester, Rochester, NY, USA, in 1984.

He is currently the Director of the Research School of Electrical, Energy and Materials Engineering, The Australian National University, Canberra, ACT, Australia. From 1985 to 2016, he was with the University of New South Wales, Sydney, NSW, Australia, where he was a Scientia Professor and an Australian Research Council Laureate Fellow with the School of Engineering and Information Technology. His main research interests include robust control theory, quantum control theory, and stochastic control theory.

Dr. Petersen was an Associate Editor for the IEEE TRANSACTIONS ON AUTOMATIC CONTROL, *Systems and Control Letters*, *Automatica*, and *SIAM Journal on Control and Optimization*. He is currently an Editor of *Automatica*. He was an Australian Federation Fellow. He is a Fellow of IFAC and the Australian Academy of Science.